Project no. 265863

ACCESS

Arctic Climate Change, Economy and Society

Instrument: Collaborative Project
Thematic Priority: Ocean.2010-1 "Quantification of climate change impacts on economic sectors in the Arctic"

D3.11 – Economic impacts of global warming on fisheries

Due date of deliverable: **31/03/2014**

Actual submission date: **18/06/2014**

Used Person/months: **19**

Start date of project: **March 1ˢᵗ, 2011**   Duration: **48 months**

Organisation name of lead contractor for this deliverable: **NOFIMA**

	Project co-funded by the European Commission within the Seventh Framework Programme (2007-2013)	
	Dissemination Level	
PU	Public	X
PP	Restricted to other programme participants (including the Commission Services)	
RE	Restricted to a group specified by the consortium (including the Commission Services)	
CO	Confidential, only for members of the consortium (including the Commission Services)	

Contents

Economic impacts of global warming on fisheries

Modelling spatial distribution of the Barents Sea cod fishery

By Arne Eide

Nofima/University of Tromsø, Norway

arne.eide@uit.no

Abstract. The paper presents a cellular automata (CA) model for the growth and spatially distribution of the Northeast Arctic cod including a harvest model based on economical rational behaviour. Rules and range of the CA model are estimated from observations and biological theory, and the environmental conditions are assumed to be in accordance with the IPCC A1B scenario for the following 45 years. The aim of the model developed is to study fleet behaviour based on avail-able management decisions, resource information and economic performance. This paper presents fleet performance in the model under open access conditions, considering two different types of vessels (small and large) placed in four different homeports. Fleet smartness is a key parameter controlling the fish finding ability of each fleet. The study shows that increasing smartness reveals increasing differences between small and large vessels placed in different homeports. While homeport clusters vessels at low levels of smartness, vessel size and range clusters vessels at higher levels of smartness.

Keywords: Economics, Open access fisheries, NEA cod, Climate change

1. Introduction

The Northeast Arctic (NEA) cod stock carries out long distance annual migrations and possesses a number of other buffering capacities enabling the stock to adapt to fluctuating environmental conditions. Climate change may cause these environmental fluctuations to exceed their normal boundaries in the years to come, making the adapting capacities of the cod stock even more important.

Previous studies suggest that management constraints may have a greater impact than climate change on the highly fluctuating Northern marine ecosystems [1], [2]. Studies also indicate that possible changes in the spatial distribution of cod and other marine organisms in the Barents Sea may be the most significant impact from cli-mate changes.

This paper aims to set up and parameterise a spatially distributed bioeconomic model of the Barents Sea cod fishery as a test bed for different management regimes and fishing strategies, including temporal and spatial variation in the fishing activities.
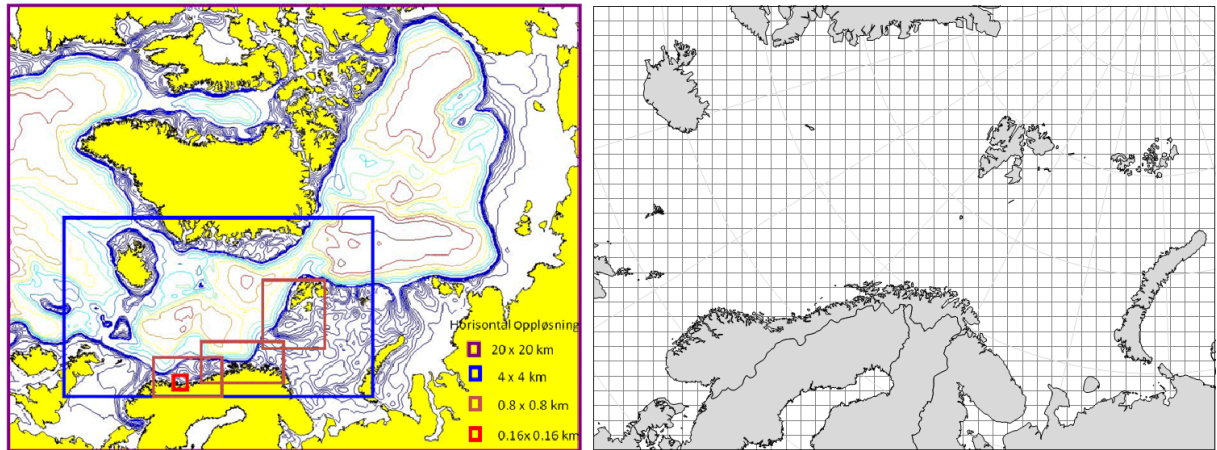
Fig. 1. Available geographical resolutions in the SinMod model (left panel) and the 80 km x 80 km grid which is used in the ecosystem model (right panel).

The time unit is one month and the spatial resolution provides a lattice of homogeneous 80 km x 80 km cells (as shown in the right panel in Fig. 1). Both temporal and spatial units are aggregated from the *SinMod* model, the latter illustrated in the left panel of Fig. 1. According to the findings of [5] cod may have a range of 210 to 720 km over a period of 30 days, indicating that 3 cells in all direction from a given cell in the grid represents a reasonable range of a cod individual during a period of one month, corresponding to the CA range 2.
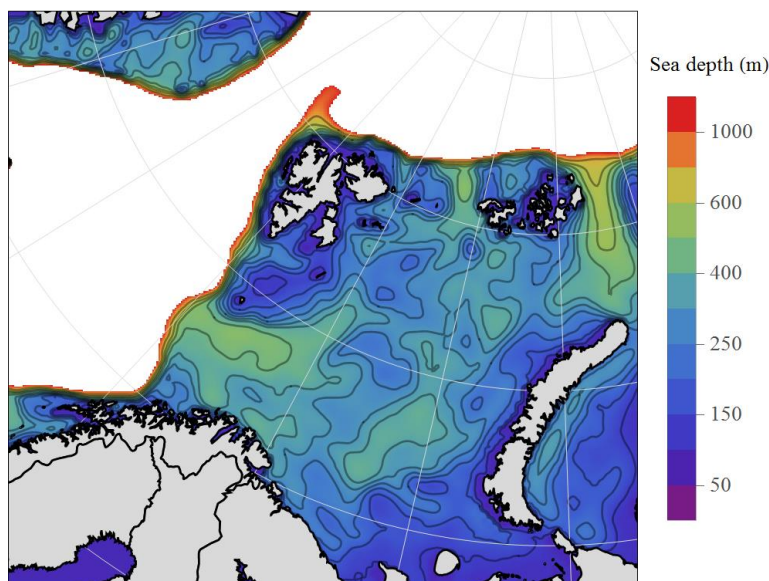

Fig. 2. Bathymetric map of the model region, the shallow water area of the Barents Sea. The white area represents ocean depths of more than 1000 meter. Source: *SinMod*.

The *SinMod* modelling project has by the courtesy of project leader Dag Slagstad provided ocean depth information (Fig. 2) and time series of spatially distributed ocean temperatures and zooplankton biomasses (Fig. 3 and 4). The time series are obtained from simulations based on the downscaled IPCC A1B scenario [6] and covers the 45 year period 2012-2057 with monthly intervals. In this study the *SinMod* data have been converted from a grid resolution of 20 km times 20 km to the model resolution (80 km times 80 km).
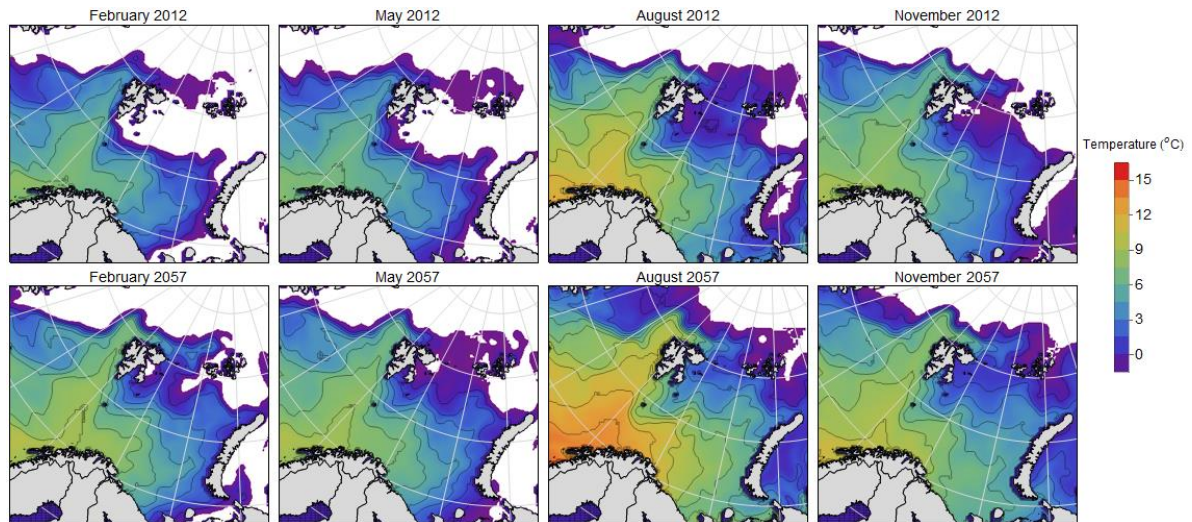

Fig. 3. Sea temperatures at 50 meter depts. In a grid resolution of 20 km times 20 km, obtained from the *SinMod* model when employing atmospheric bordering conditions downscaled from the IPCC A1B scenario. The panels show the mid-month of each quarter the first (2012) and last year (2057) of the simulations. Areas with temperatures below -1.5 oC are left out (indicated by white area).
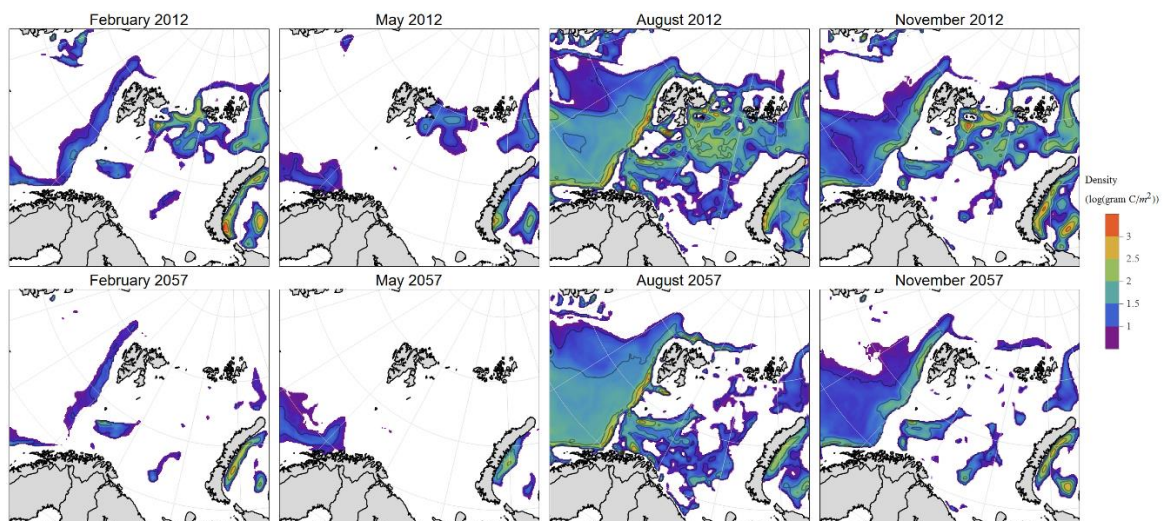
Fig. 4. Spatial distribution of zooplankton densities (biomasses) calculated by *SinMod* simulations while running the downscaled version of the IPCC A1B scenario. The panels show the mid-month of each quarter the first (2012) and last year (2057) of the simulations. Zooplankton densities below 2 g C/m2 are shown as white areas. A log scale is used in the figure.

Temperatures considered are average monthly values at depths of 50 meter. Zoo-plankton biomasses are aggregated biomasses including several species, all characterised by being spatially determined by physical processes and nutrients availability, in contrast to living organisms at higher trophic levels where individual behaviour of the species significantly influence the spatial distribution.

The carrying capacity in terms of potential cod biomass each cell can hold in each month throughout the considered period is assumed to depend on biological and physical environmental conditions within the cell, represented by the A1B scenario through inputs from the *SinMod* model (Figures 2, 3 and 4).
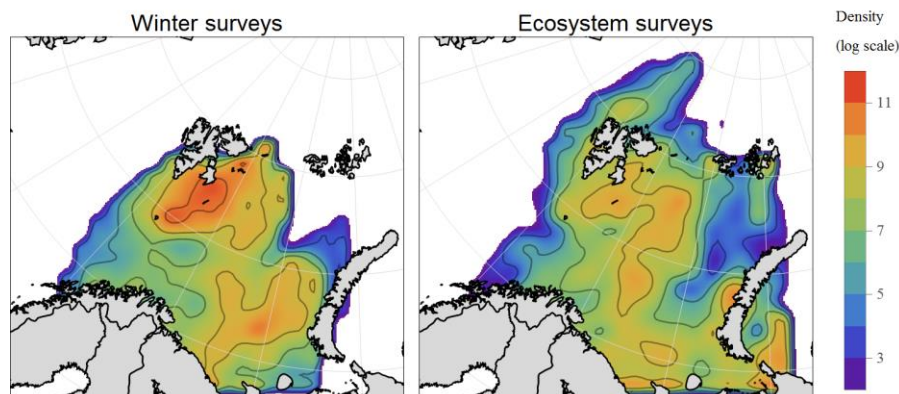
Fig. 5. Normalised spatial distributions of NEA cod as it appears in winter and ecosystem surveys aggregated over the years 2004-2010. The distributional charts are calculated by interpolating and integrating *FishExChange* data. A logarithmic scale presents densities.

Information on spatial distribution of NEA cod for the period 2004-2010 is provided by the *FishExChange* project. Catches are registered on a quarterly basis while the surveys take place once a year, winter surveys in April/May and ecosystem surveys in August/September. Age structured data has been aggregated for the purpose of this study. Registered catches are interpolated spatially by Radial Basis Function (RBF) interpolation [7] and the interpolated surface is integrated and distributed on an equal size geographic grid as shown in Fig. 1 based on equal size projection (Lambert Azimuthal, corresponding to the projection used in the *SinMod* model, coordinates origin in 60N, 58E). Resulting spatially distributed biomasses and catches are shown in Fig. 5 and 6.
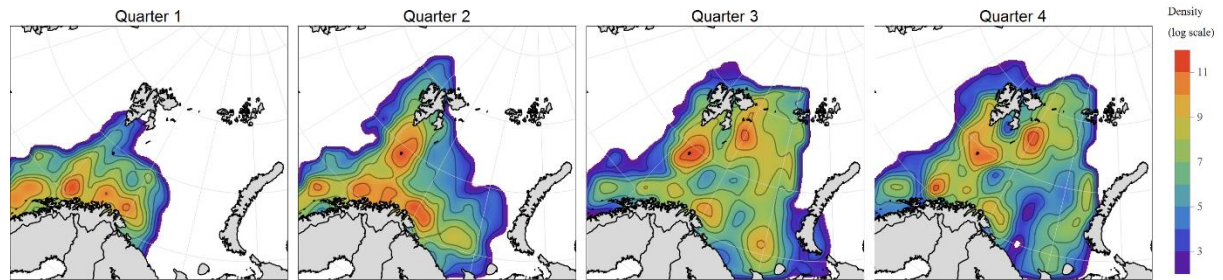
Fig. 6. Normalised quarterly spatial distributions of NEA cod catches aggregated over the years 2004-2009. The distributional charts are calculated by interpolating and integrating FishExChange data. Densities are presented by a logarithmic scale. Densities are presented by a logarithmic scale.

# 2. Temporal and spatial distribution of carrying capacities

The different sources providing information about the spatial distribution of cod represent different sampling methods and different aims. The catch information obviously gives a biased overall distribution since the most profitable areas are expected to be overrepresented. Further are surveyed areas constrained and may exclude cod dense areas, as for example spawning grounds and other coastal areas in the winter surveys. The assumed monthly spatial distributions of the cod stock are estimated by the different data sources according to the weights presented in Fig. 7.

The top row of Fig. 8 shows the weighted distribution charts of carrying capacities for selected months of the first year (2012). The distribution areas are directly drawn from normalised catches, surveys and ocean depts.
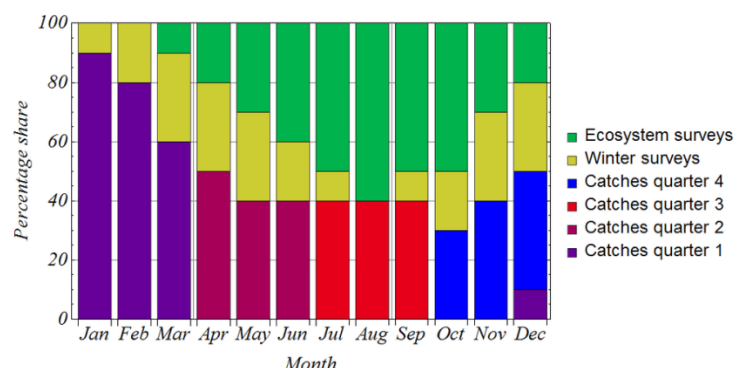
Fig. 7. The composition of six different sources of distributional information (covering the period 2004-2009/2010) for constructing overall distributional charts on a monthly basis.
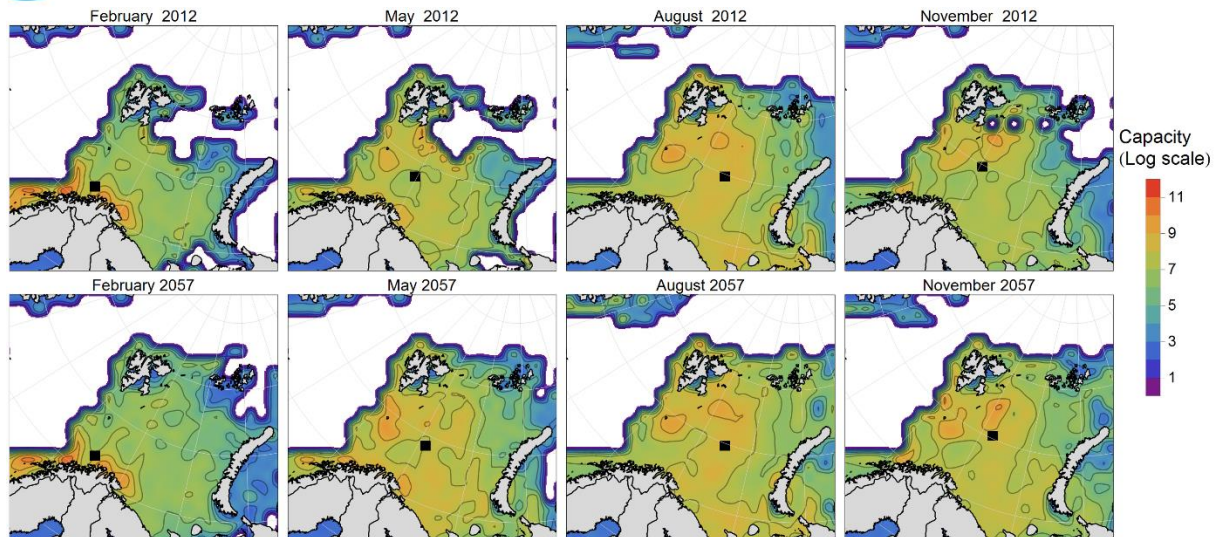
Fig. 8. Spatial distribution of environmental carrying capacities for NEA cod the first (2012) and last (2057) or the performed simulations. The distribution is based on different sources of spatial distribution of NEA cod during the period 2004-2010, ocean temperatures and zooplankton biomasses from *SinMod* (A1B scenario runs) and ocean depths. The monthly centres of gravity for the levels of carrying capacities are shown as black squares. The size of each square corresponds to the grid resolution (80 km times 80 km, see right hand panel of Fig. 1).

The bottom row of Fig. 8 is based on assumed changes in the distributional pattern (carrying capacity levels) caused by changes in temperatures (Fig. 3) and zooplankton production patterns (Fig. 4). Together with ocean depths (Fig. 2) and the initial migration pattern (Fig. 10), these are essential factors for the distribution of cod.

The following assumptions have been implemented in the calculation of changing carrying capacities: NEA cod distribution is constrained to ocean depths less than 1000 meter (Fig. 2) and ocean temperatures (average at 50 meter depth) higher than -1.5 $^{\circ}$C (Fig. 3). In addition, environmental carrying capacities are reduced by 80% when zooplankton densities fall below 2 g carbon per square meter (Fig. 4).
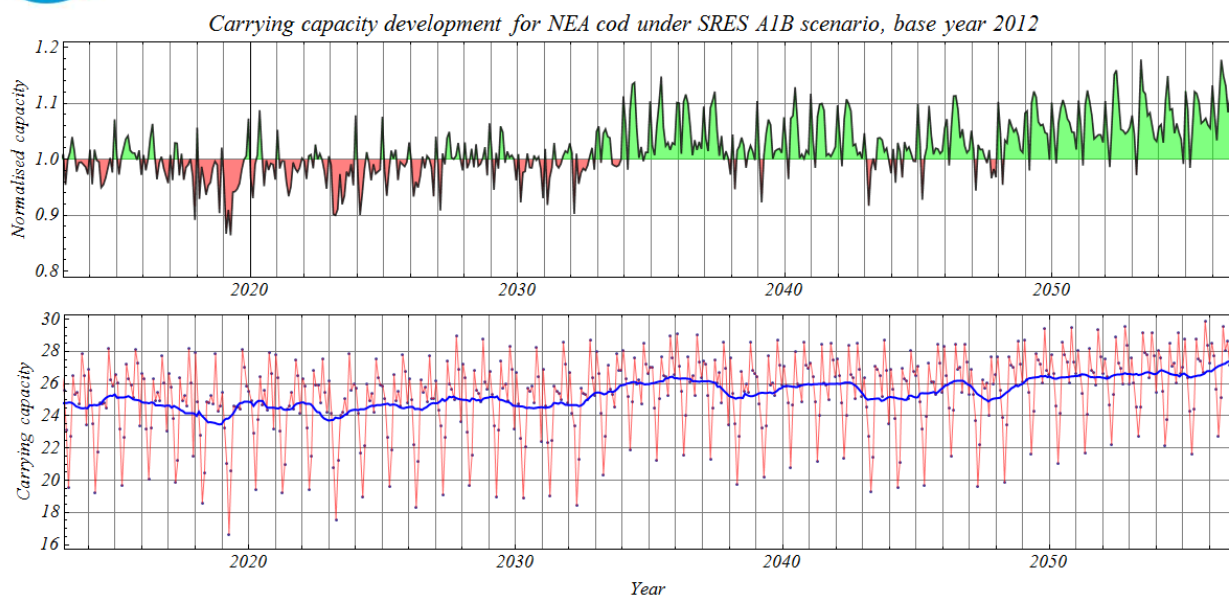
Fig. 9. The upper panel shows monthly aggregates of normalised (base year 2012) carrying capacities for NEA cod based on *SinMod* A1B simulations and initial distribution data from the *FishExChange* project (2004-2010). The anomalies show percentage deviation from corresponding month in 2012. The lower panel shows the monthly changes in terms of total carrying capacities of all cells (in million tons cod biomass). The red curve gives the monthly variation while the blue curve is the 12-month moving average of these numbers.
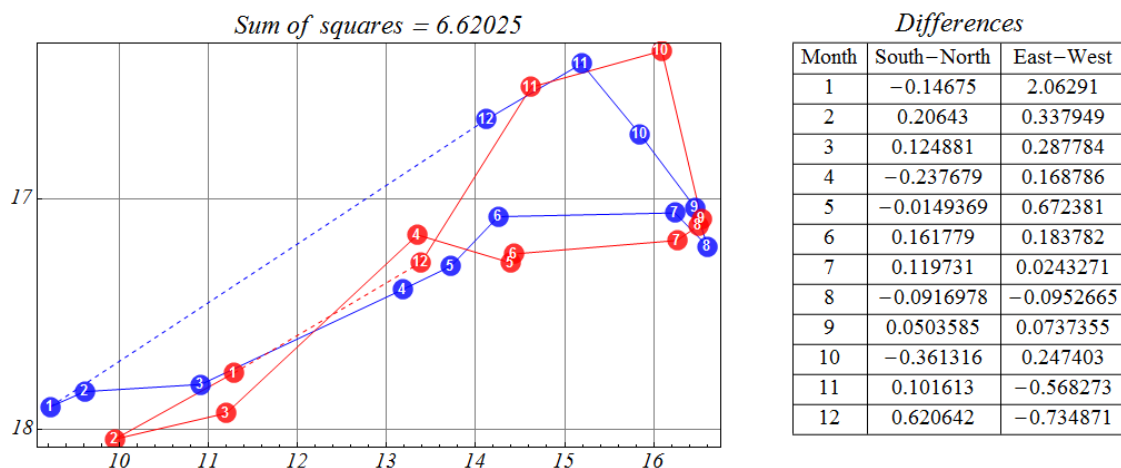
Centres of gravity of the potential spatially distributed biomass of NEA cod (the black squares shown in Fig. 8) indicate insignificant changes in spatial distribution of cod over the 45-year period (2012-2057). Centres of gravity only move one cell (80 km) sideways (to the right, indicating eastward and slightly northward movement) the first and last quarters of the year when comparing the situations in 2012 and 2057 (Fig. 8). A more careful look on the monthly centres of gravity confirms this. Fig. 12 shows monthly distributions of centres of gravity placed into the model lattice in selected years. The changes over the 45-year period are insignificant and the intra-annual variation is always constrained by the same rectangular limiting borders.

Spatially aggregated monthly carrying capacities (summing up cell capacities in the distribution area) over the 45-year period indicate a slight decline by about 2017-2018, thereafter normalising to 2012-level in the end of the 2020s before increasing in the mid-2030s. The high values remain towards the end of the period (Fig. 9).

3. CA model of cod growth and biomass distribution

A cellular automata (CA) model following the set up in [8] is implemented for the NEA cod stock, based on historical growth and spatial distribution pattern represented by the current climatic conditions. The CA rules utilise Moore neighbourhoods of range 2, a spatial resolution of 80 x 80 km and a temporal resolution of one month.

Distribution rules are identified by fitting modelled migratory pattern to the current capacity data, representing the annual variation in the NEA Cod stock distribution. The biological CA rules (which could be interpreted as migration matrices) are found by an algorithm minimising sum of squared distances between actual (Fig. 8, upper row) and modelled centres of gravity of spatial distribution of cod under current cli-mate conditions. Fig. 10 shows the observed migration pattern (in blue) and the modelled pattern (in red). Fig. 12 displays monthly centres of gravity in different years as obtained by the estimated CA rules (Fig. 11) after implementing the A1B scenario.

| Month	South−North	East−West
1	−0.14675	2.06291
2	0.20643	0.337949
3	0.124881	0.287784
4	−0.237679	0.168786
5	−0.0149369	0.672381
6	0.161779	0.183782
7	0.119731	0.0243271
8	−0.0916978	−0.0952665
9	0.0503585	0.0737355
10	−0.361316	0.247403
11	0.101613	−0.568273
12	0.620642	−0.734871

Fig. 10. Estimated (blue) and modelled (red) centres of gravity of the spatial distribution of cod. The modelled centres of gravity are obtained by numerically minimising the sum of square distances between actual and modelled centres of gravity. The final distances are shown as differences in the table.

The procedure described above is first carried out for a growth rate believed to be within the range of the actual growth. Then the growth rate was calibrated on the basis of assumed maximum biomass level (in its natural state, without fishing, this level is assumed to be twice the observed maximum level of 4 million tons [9], and growth; before repeating the procedure until estimated universal gross growth rates converge to 11% per month. This growth rate is not to be confused with the marginal growth of individuals (e.g. the growth rate of a von Bertalanffy equation) or the intrinsic growth rate

of a surplus production function. Adjusted by local collapses [8] the net growth also has a spatial dimension as the net growth varies both temporally and spatially, influenced by the migration pattern but also changes in local capacities controlling the occurrence of local biomass collapses.
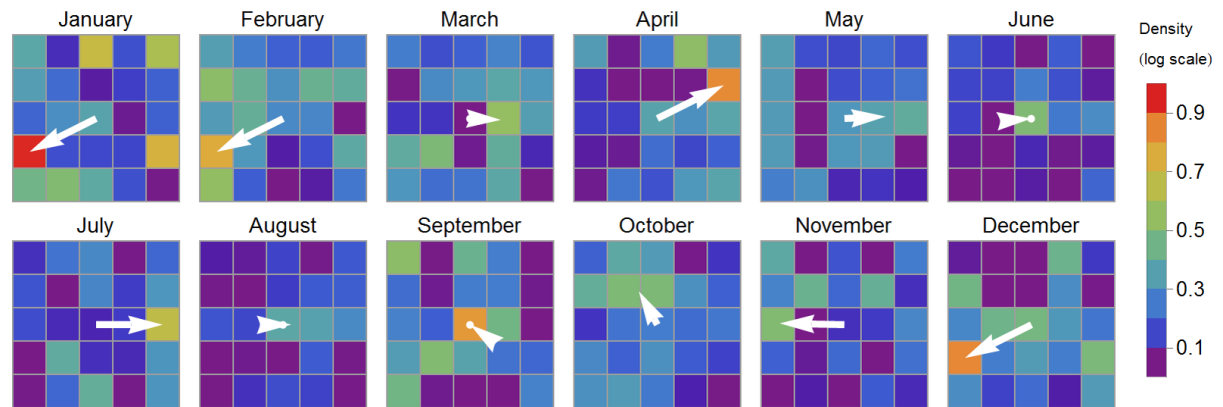
Fig. 11. CA rules (migration patterns) when assuming Moore neighbourhoods with a range of 2 (cells). The figures indicate monthly diffusion into neighbouring cells from the centre cell and the arrows (vectors) show the average direction and intensity of the migration.
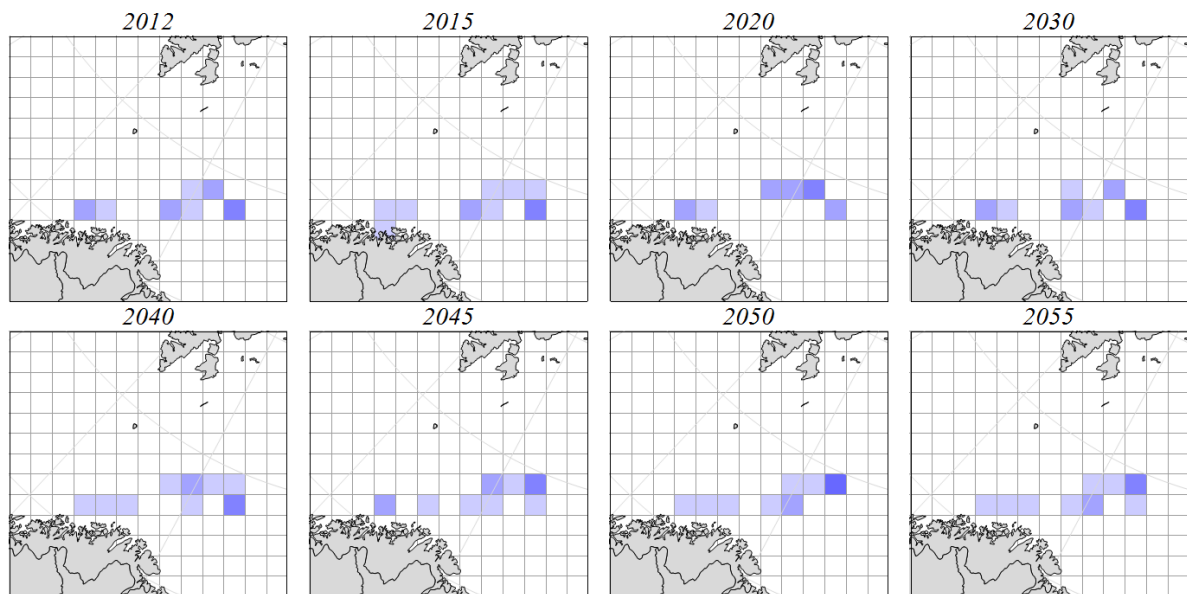
Fig. 12. Monthly centres of gravity in the cod stock distribution for selected years 2012 – 2055 based on the A1B scenario capacity data for an unexploited cod stock. Darker cell colour indicates that the cell is centre of gravity in two or more months the selected year. Grid size and geographical orientation is extracted from the right hand panel in Fig. 1.

Unlike the universal gross growth rate, the carrying capacity of each cell varies by temperature and food availability, by which also the net growth rate is affected. The biological model utilises physical and biological data provided by *SinMod* simulations, serving as proxies for these factors in the model. The carrying capacity of a cell influences net growth through increasing mortality when carrying capacity decreases (causing a higher frequency in local collapses when all other factors remain constant).

It is already possible to make an important conclusion from the model, illustrated by Fig. 12 in which monthly centres of gravity of cod biomass are pictured for selected years up to 2055. There are no signs of significant climate driven changes in cod distribution over this period of 45 years.

4. Open access fishery

The fishery is assumed to largely follow the model presented in [8]. Monthly vessel catches (h) are distributed on different cells according to available biomass in each cell (*x*), a fleet specific catchability coefficient (*q*), fleet specific stock-output elasticity (*β*) and the fishing effort produced by the fleet in the actual cell during a period of one month (*e*). A Cobb-Douglas harvest function is assumed [10], the harvest in cell *i* is then given by

$$h_i(e_i, x_i) = q\, e_i\, x_i^{\beta} \tag{1}$$

Let E_t be the total fishing effort of all cells at month *t*, summing up each effort within each cell in a total of *n* cells:

$$E_t = \sum_{i=1}^{n} e_{i,t} \tag{2}$$

While E_t is the total fishing effort produced by the fishing fleet during month *t*, the fleets total capacity of producing effort could be higher. Let the theoretical maximum level of effort production be F_t. The produced fishing effort is then constrained by

$$0 \le E_t \le F_t \tag{3}$$

Capacity utilisation (*E/F*) is determined by expected economic performance and, if existing, constraining regulations. Without regulations, the fleet will fish if it is economically beneficial for the fleet to fish. If the expected income from the fishing operation is not covering the running costs, the fleet will stay in harbour. The income function of the fishery in cell *i* (re_i) assumes a constant unit price of harvest (*p*):

$$re_i(e_i, x_i) = p\, h_i(e_i, x_i) \tag{4}$$

Running costs of the fishery in cell i is given by the fishing effort in the cell (e_i) and the measured distance (d_i) from the homeport of the fleet to the centre of the cell where fishing takes place. The variable cost function (vc_i) includes two parameters: c_e (constant unit cost of fishing effort) and c_d (effort cost of distance):

$$vc_i(e_i, d_i) = (c_e + c_d d_i)\, e_i \tag{5}$$

The contribution margin of the fishery for a given fleet (adding the month indexes, *m*, for all cell variables) within the available area of the fleet is obtained by

$$cm(\boldsymbol{e}, \boldsymbol{x}, \boldsymbol{d}) = \sum_{m=1}^{12} \sum_{i=1}^{n} \{re_{m,i}(e_{m,i}, x_{m,i}) - vc_{m,i}(e_{m,i}, d_{m,i})\} \tag{6}$$

when the variables ($\boldsymbol{e}, \boldsymbol{x}, \boldsymbol{d}$) represent respectively the matrices ($e_{m,i}, x_{m,i}, d_{m,i}$) for $i \in [1, n]$ and $m \in [1,12]$. Annual net revenue in the same fishery is

$$\pi(\boldsymbol{e}, \boldsymbol{x}, \boldsymbol{d}) = cm(\boldsymbol{e}, \boldsymbol{x}, \boldsymbol{d}) - fc \tag{7}$$

when fc is the fixed cost per vessel.

While the fleet economy in the short run will determine fleet utilisation (*E/F*), previous economic performance also influences future effort producing capacity of the fleet (*F*), which will increase or decline depending on economic performance in a speed determined by the assumed entry/exit rates of the fleet. In this model entry and exit rates (fg and fd respectively) are independently given as exogenous parameters.

When including the opportunity costs of labour and capital in c_e, c_d and fc, normal profit is embedded as a cost component. Equation (7) therefore represents economic rent or abnormal profit in the fishery. In an open access fishery then the sign of $\pi(\boldsymbol{e}, \boldsymbol{x}, \boldsymbol{d})$ determines growth and decline in the fleet size (*F*, the capacity of effort production) over time according to the following rules:

$$\begin{aligned} If \quad &\pi(\boldsymbol{e}, \boldsymbol{x}, \boldsymbol{d}) < 0 \quad then \quad F_{t+1} = (1 - fd)F_t \\ If \quad &\pi(\boldsymbol{e}, \boldsymbol{x}, \boldsymbol{d}) > 0 \quad then \quad F_{t+1} = (1 + fg)F_t \end{aligned} \tag{8}$$

Because of temporal and spatial variation of fish biomasses, also revenues and costs of fishing in different areas (cells) varies in time and by area. Fishers are assumed to target the cells of the highest revenue-cost ratios given the information available. Without any prior knowledge about potential costs and revenues, it may be argued that it is rational to distribute the effort uniformly in the available area (the area within range of the vessel).

Because of temporal and spatial variation of fish biomasses, also revenues and costs of fishing in different areas (cells) varies in time and by area. Fishers are assumed to target the cells of the highest revenue-cost ratios given the available information. Without any

prior knowledge about costs and revenues, it may be argued that it is rational to have a uniform distribution of effort in the area within range of the fleet. $e_{i,t}$ is the fishing effort of cell i at time t. With n available cells, uniform distribution of effort gives a fishing effort of $e_{i,t} = \frac{E_t}{n}$ in all available cells in month t.

This relates to the assumed revenue-cost ratio by the introduction of a smartness (or effort distribution) parameter $s = 0$. s reflects increasing knowledge on costs and revenues potentials (including fish finding abilities) by increasing value of s. Assume the distribution of effort within the lattice to be given by

$$e_{j,t} = \frac{\left(\frac{re_{j,t}}{vc_{j,t}}\right)^s}{\sum_{i=1}^{n}\left(\frac{re_{i,t}}{vc_{i,t}}\right)^s} E_t \tag{9}$$

5. Results

Obviously uniform distribution of effort is obtained by s = 0 in equation (9), while s = 1 gives an effort distribution perfectly reflecting the distribution of revenue-cost ratios. Increasing s-values reflect increasing ability to identify the most profitable cells. As s approaches infinity all effort moves into the single cell with marginal higher ratio than any other cell.

Monthly changing biological CA rules (Fig. 11) and the dynamic interaction be-tween biological processes and open access fleet dynamics lead to pseudo-random patterns causing fluctuating quantities of quasi rent in the fleet over time. [1], [2] show that the flow of quasi rent in open access fisheries may even exceed the ab-normal profit obtained in a regulated fishery. The following example indicates how climate change may affect the fishery on the equally shared Russian and Norwegian NEA cod stock, in a situation of pure open access dynamics.

The fleet dynamics of the Norwegian cod fishery is modelled in larger details while a corresponding catch quantity is assumed obtained by Russian vessels in the area available for the Russian fleet. The assumed distribution of Russian catches follow the distribution of cod biomasses in the relevant area.

The Norwegian fleet consists of two different vessel types (small and large vessels) placed in four different homeports: Svolvær, Tromsø, Hammerfest and Vardø (Fig. 13). The initial number of vessels is identical in each port, with the same number of small and large vessels. Each type of vessels (small and large) has the same techno-logical

efficiency, price on harvest and cost functions independent of homeport (for more details please contact the author).
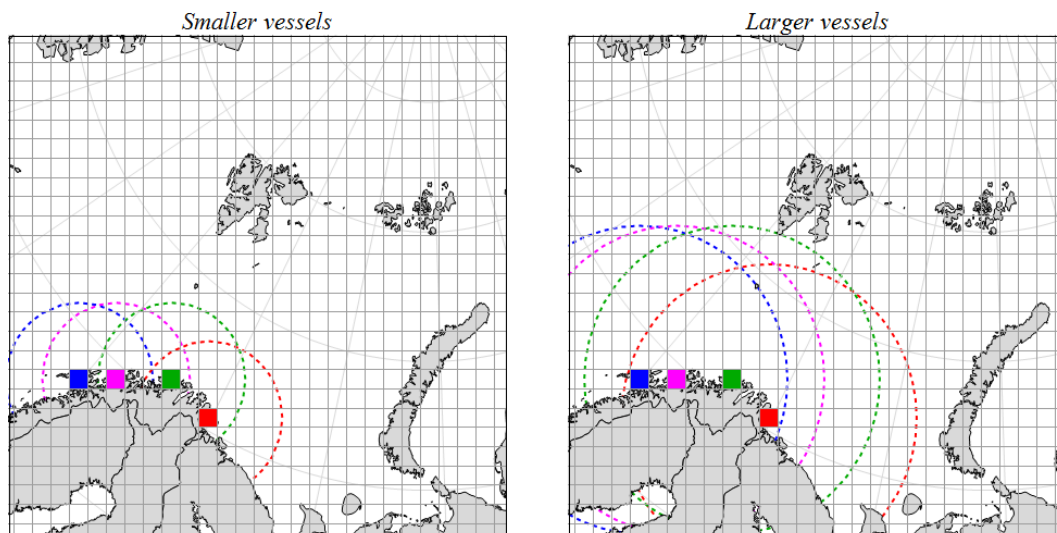
Fig. 13. The maps shows four Norwegian fishing ports: Svolvær (blue), Tromsø (magenta), Hammerfest (green) and Vardø (red); and monthly ranges of two fleets (smaller and larger vessels) placed in each port. The fleet range from the centre of the homeport cell is four squares (cells) for the smaller vessels and eight squares for the larger vessels.
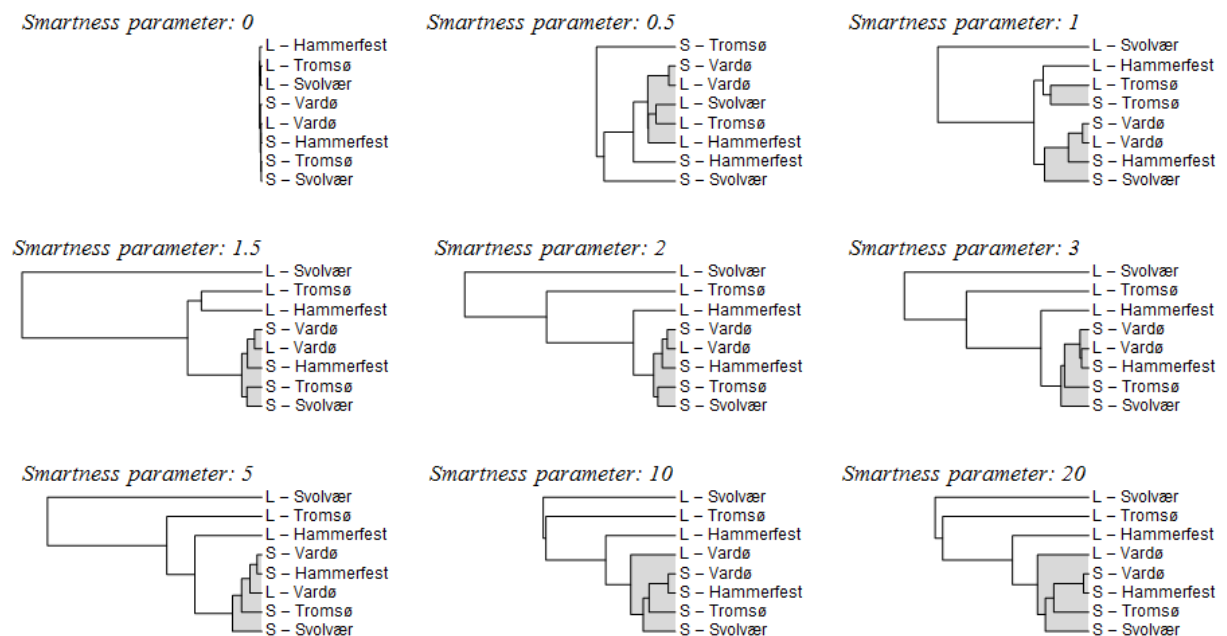
Fig. 14. Dendrogram plots of performance relations between small (S) and large (L) fishing vessels operating from four different North-Norwegian homeports (Svolvær, Tromsø, Hammerfest and Vardø) for different values of the smartness-parameter s. Clustering level 5 is shaded.

Simulations covering the 45-year period (2012-2057) where performed for nine different smartness parameter (s in equation 9). The selected values of s were 0, 0.5, 1, 1.5, 2, 3, 5, 10 and 20. A priori *s*-values below 1 is rather unlikely. The upper limit of *s* is more difficult to identify, but it seems reasonable to expect the value to be within the interval of 1 and 10, representing a wide range of possible outcomes.

The simulations generate a large number of data, covering biological and economic performance, spatially and temporally. Fleet differences are illustrated in Fig.14 in terms of dendrogram plots of fleet clusters. The clustering scales (horizontal axes) are fixed, e.g. the clustering patterns of different s-values are comparable.

6. Conclusion

As expected uniform distribution of effort (s = 0) does not reveal any performance differences between the vessels (Fig. 14). At s = 0.5 large vessels in all homeports cluster slightly and clearly more than the smaller vessels. However, as the s-value increases beyond one, the tendency of clustering among small vessel also increases, while this is not the case for the large-scale vessels.

Another pattern displayed in Fig. 14 is a clustering tendency on homeport rather than vessel type at low s-values (particularly strong for the Vardø-fleet) while type of vessel (small and large) seems to be an increasingly more important clustering factor as the s-value becomes higher. This seems reasonable, since increased smartness (e.g. fish-finding capacity) to some extent may compensate for geographical disadvantages. It is however surprising that this effect tends to be stronger for the smaller vessels than for the larger.

Test simulations without climate change show a large degree of correspondence with the results presented above, even though measured cluster differences are less pronounced than those shown in Fig. 14. This indicates that today's marginal differences between fleet segments could increase because of changing climatic conditions. The most important conclusion is however, that technological development and changes in fleet performance, in addition to choice of management regime, could potentially have a stronger impact on the economic performance of Northern fisheries than climate change may have.

7. References

1. Eide, A.: Economic impacts of global warming. The case of the Barents Sea fisheries. Natural Resource Modeling 20(2):199–221 (2007)

2. Eide, A.: An integrated study of economic effects of and vulnerabilities to global warming on the Barents Sea cod fisheries. Climatic Change 87(1): 251–262 (2008)

3. Jacob D, Andrae U, Elgered G, Fortelius C, Graham LP, Jackson SD, Karstens U, Koepken C, Lindau R,Podzun R, Rockel B, Rubel F, Sass HB, Smith RND, van den Hurk BJJM, Yang X.: A comprehensive model intercomparison study investigating the water budget during the BALTEXPIDCAP Period. Meteorol Atmos Phys 77:19–43 (2001)

4. Slagstad, D., & McClimans, T. A.:. Modeling the ecosystem dynamics of the Barents sea including the marginal ice zone: I. Physical and chemical oceanography. Journal of Marine Systems 58(1):1–18 (2005)

5. Rose, G.A., B. deYoung, and E.B. Colbourne: Cod (*Gadus morhua*) migration speeds and transport relative to currents on the North-East Newfoundland Shelf. ICES J. Mar. Sci. 52: 903– 914 (1995)

6. Nakícenovíc N, Alcamo J, Davis G, de Vries B, Fenhann J, Gaffin S, Gregory K, Grübler A, Jung TY, Kram T, Emilio la Rovere E, Michaelis L, Mori S, Morita T, Pepper W, Pitcher H, Price L, Riahi K, Roehrl A, Rogner H-H, Sankovski A, Schlesinger ME, Shukla PR, Smith S, Swart RJ, van Rooyen S, Victor N, Dadi Z.: Special report on emissions scenarios. Cambridge University Press, Cambridge, 599 pages (2000)

7. Myers, D. E.: Spatial interpolation: an overview. Geoderma 62(1):17-28 (1994)

8. Eide, A.: On the limits of improved fish finding capacity and its contribution to resource conservation. In Chan, F., Marinova, D. and Anderssen, R.S. (eds) MODSIM2011, 19th International Congress on Modelling and Simulation. Modelling and Simulation Society of Australia and New Zealand, December 2011, MODSIM2011 2493-2499. ISBN: 978-0-9872143-1-7. Available at http://www.mssanz.org.au/modsim2011/E16/eide.pdf (2011)

9. Lilly, G. R., Wieland, K., Rothschild, B. J., Sundby, S., Drinkwater, K., Brander, G. Otter-sen, J.E. Carscadden, G.B. Stenson and G.A. Chouinard: Decline and recovery of Atlantic cod (Gadus morhua) stocks throughout the North Atlantic. In G. H.Kruse, K. F.Drinkwater, J. N.Ianelli, J. S.Link, D. L.Stram, V.Wespestad, and D.Woodby (eds.): Resiliency of gadic stocks to fishing and climate change, Alaska Sea Grant, University of Alaska, Fairbanks, pp. 39–66 (2008)

10. Eide, A., Skjold, F., Olsen, F. and Flaaten, O.: Harvest Functions: The Norwegian Bottom Trawl Cod Fisheries, Marine Resource Economics 18: 81–93 (2003)